Supporting Information

Nanoscale Observation of Solid Electrolyte Interface and Lithium Dendrite Nucleation-Growth Process during Initial Lithium Electrodeposition

Shuwei Wang[a,b], Xiaoguang Yin[a,c], Dongqing Liu[a,d]*, Yuanming Liu[a], Xianying Qin[a], Wei Wang[a,b], Rui Zhao[a,b], Xiaojie Zeng[a,b], Baohua Li[a]*

[a] Shenzhen Key Laboratory on Power Battery Safety Research and Shenzhen Geim Graphene Center, Tsinghua Shenzhen International Graduate School, Shenzhen 518055, China

[b] Laboratory of Advanced Materials, School of Materials Science and Engineering, Tsinghua University, Beijing 100084, China

[c] School of Environmental Science and Engineering, Southern University of Science and Technology, Shenzhen, 518055, China

[d] College of Mechatronics and Control Engineering, Shenzhen University, Shenzhen, 518060, China

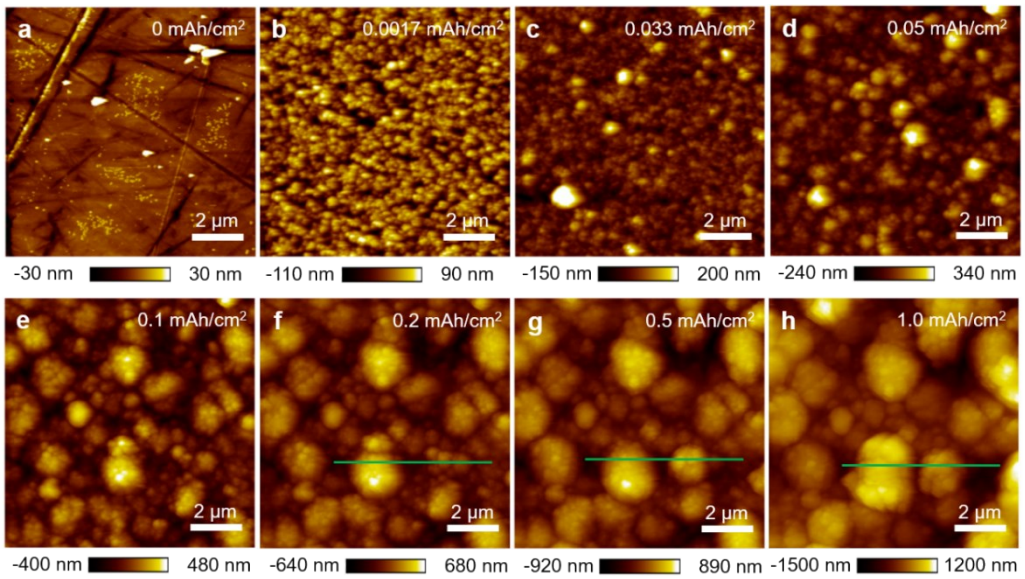

Figure S1. In situ EC-AFM images of the interfacial evolution during the deposition process at current density of 0.5 mA/cm^2 (a-h).

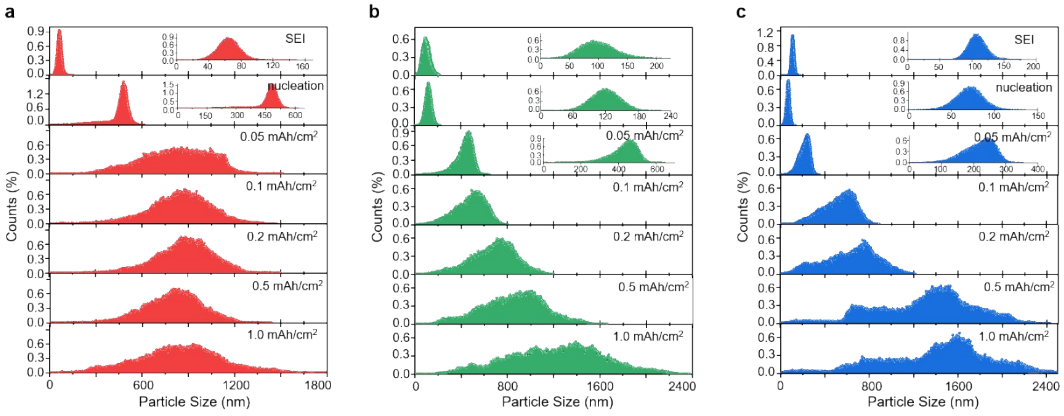

Figure S2. Depth distribution of the particles during lithiium deposition at different current densities of (a) 0.2 mA/cm^2, (b) 0.5 mA/cm^2 and (c) 1.0 mA/cm^2.

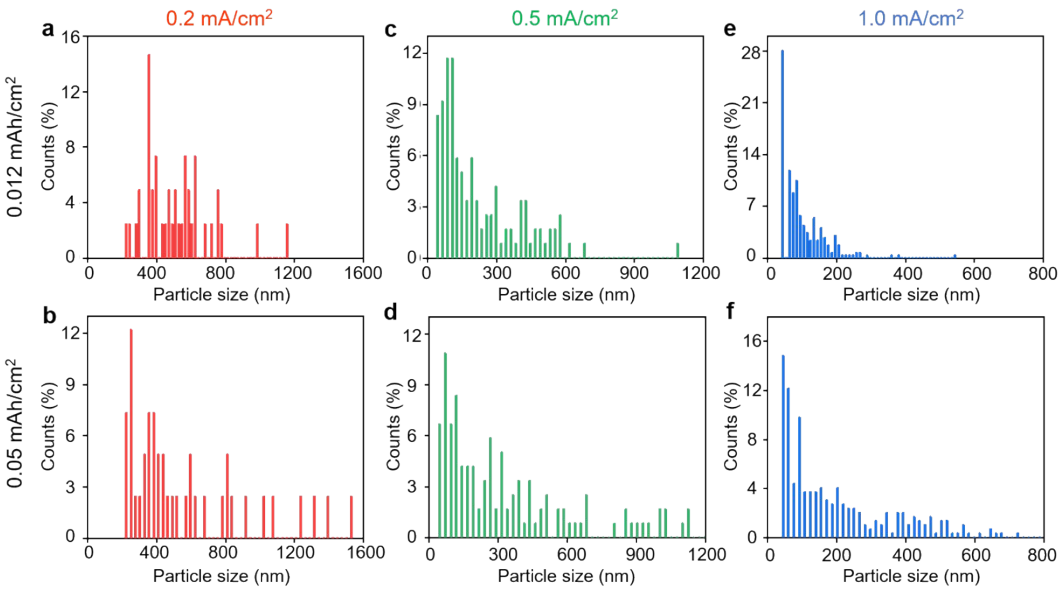

Figure S3. The particle diameter histogram of Figure 2 (b) at different current densities of 0.2 mA/cm^2(a-b), 0.5 mA/cm^2(c-d) and 1.0 mA/cm^2(e-f) during lithium nucleation.

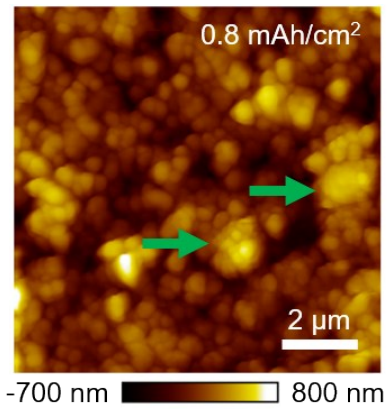

Figure S4. The AFM images of Cu anode after deposition capacity of 0.8 mAh/cm^2 at 0.2 mA/cm^2.

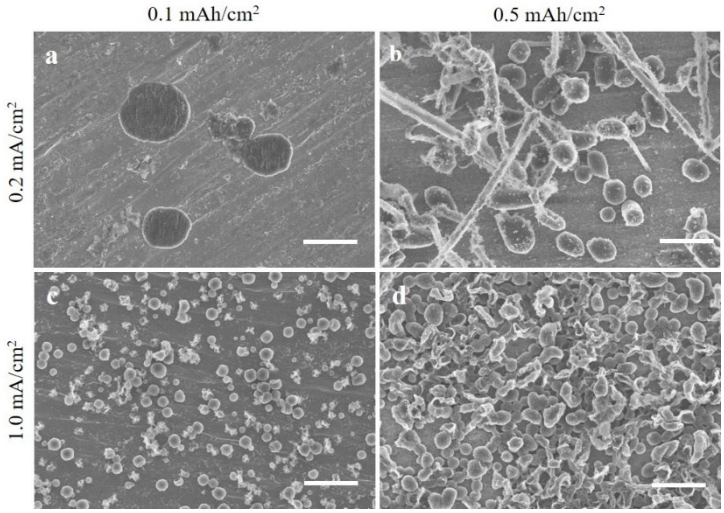

Figure S5. Lithium deposition at current densities of 0.2 mA/cm^2 (a)(b) and 1.0 mA/cm^2 (c)(d): 0.1 mAh/cm^2 for (a)(c); 0.5 mAh/cm^2 for (b)(d). The scale bar is 10 μm.

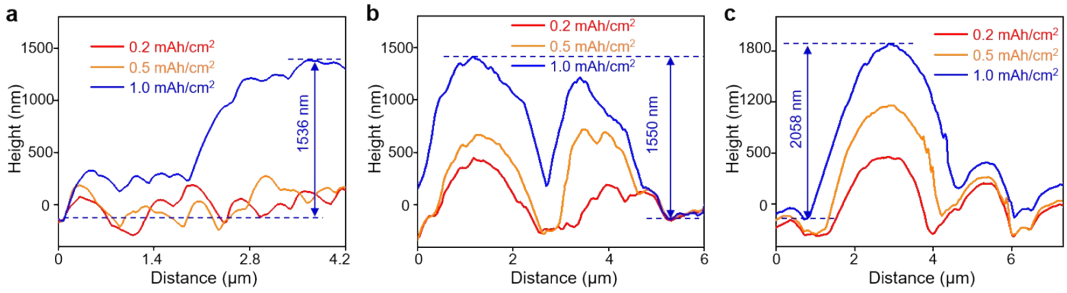

Figure S6. The corresponding height curves in corresponding to the marked regions in the in situ AFM images at different current densities of 0.2 mA/cm^2, 0.5 mA/cm^2, and 1.0 mAh/cm^2.

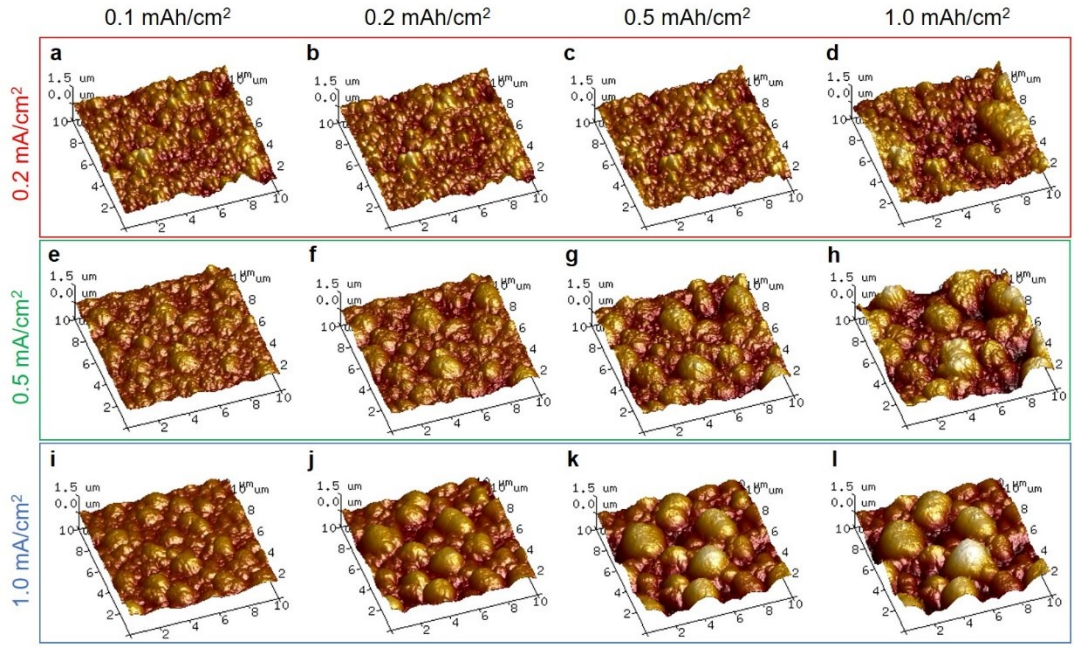

Figure S7.. In situ 3D AFM images of the interfacial evolution during deposition process at current densities of 0.2 mA/cm^2 (a-d), 0.5 mA/cm^2 (e-h), and 1.0 mA/cm^2 (i-l).

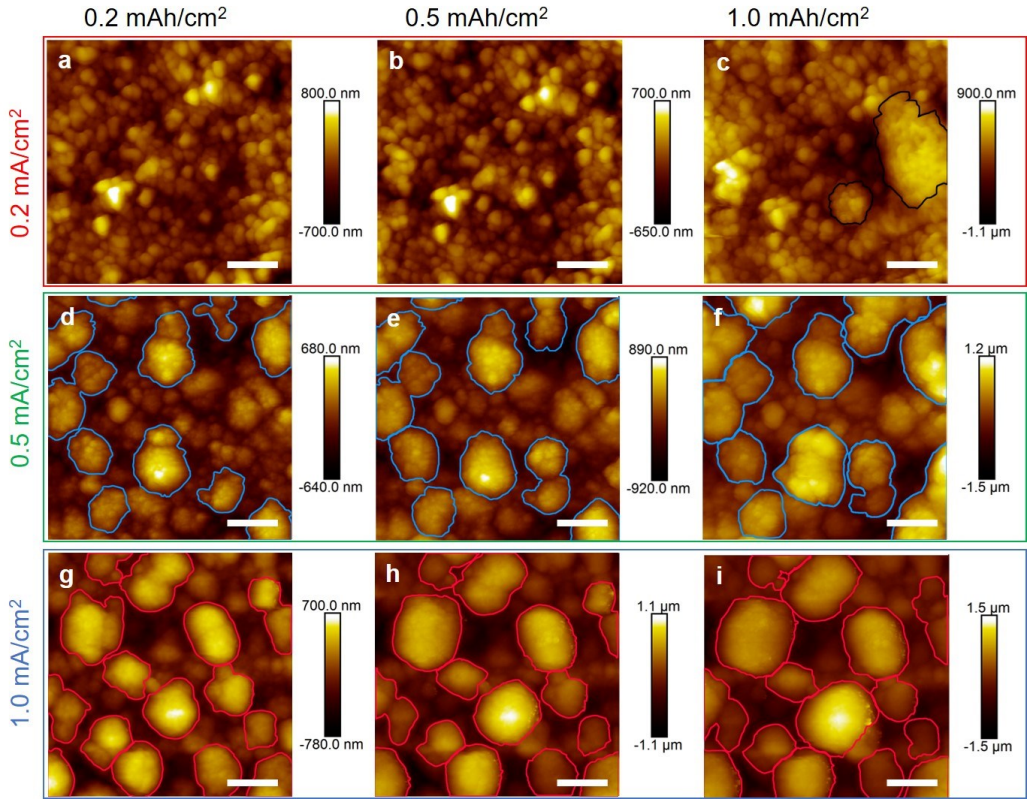

Figure S8. The protrusion analysis to quantify the area of protrusion changes during the deposition at current densities of 0.2 mA/cm^2 (a-c), 0.5 mA/cm^2 (d-f), and 1.0 mA/cm^2 (g-i).

Simulation notes: A 2D domain of 11 μm × 2 μm is constructed for the initial nucleation stage simulation, as shown in Figure S9a. A surface with 2 μm × 2 μm bumps is constructed to exemplify the effect of Li ion transport on the deposition geometry in Figure S9b. The bottom boundary potential is grounded, and the average current density boundary condition is applied at the top boundary. Symmetric boundary conditions are assigned at two side boundaries. For the initial nucleation stage simulation, the electrolyte concentration is set as 10^3 mol/m^3, the diffusion coefficient is 2×10^{-9} m^2/s, and the reduction reaction overpotential sine function has a wavelength of 2 μm. For the growth stage simulation, to emphasize the effect of lithium ion transport, the initial electrolyte concentration is set as 500 mol/m^3, and the diffusion coefficient is 5×10^{-12} m^2/s. An artificial layer with low constant conductivity and position-dependent thickness is added at the electrolyte/electrode interface to mimic the SEI.

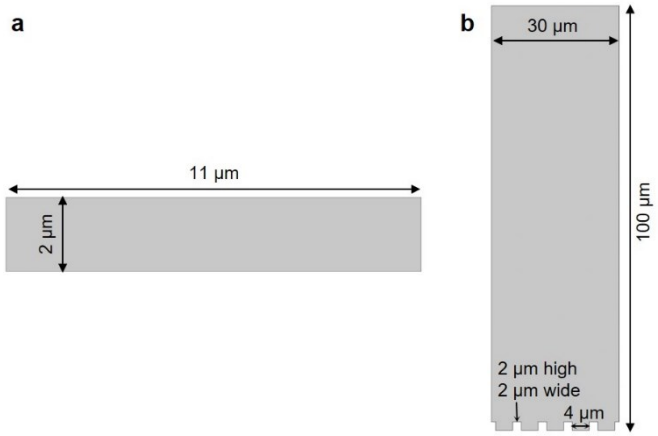

Figure S9. (a) Geometry for the initial reaction-controlled nucleation stage simulation and (b) transport-controlled early growth stage simulation. Figure (a) and (b) are not illustrated with the same length scale.

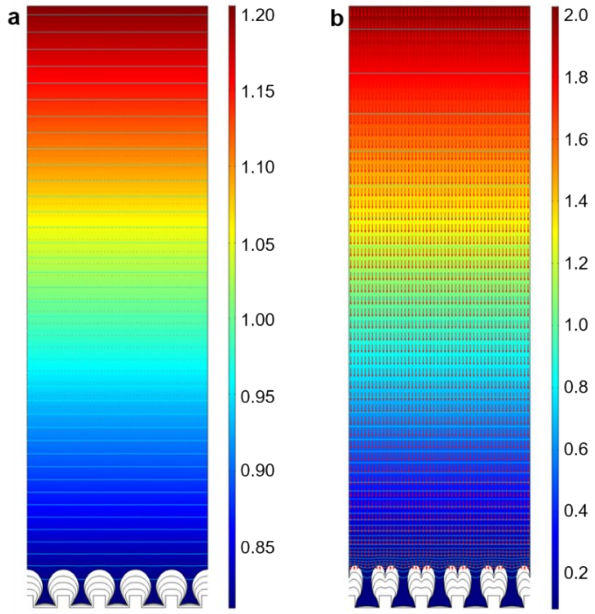

Figure S10. Normalized concentration distribution (color scale bar) inside domain and deposition geometries (bottom) after deposition at current densities of (a) 0.2 mA/cm^2 and (b) 1.0 mA/cm^2 for total capacities of 0.5 mAh/cm^2, 1.0 mAh/cm^2, 1.5 mAh/cm^2 and 2.0 mAh/cm^2. The ion flux are given by arrows.

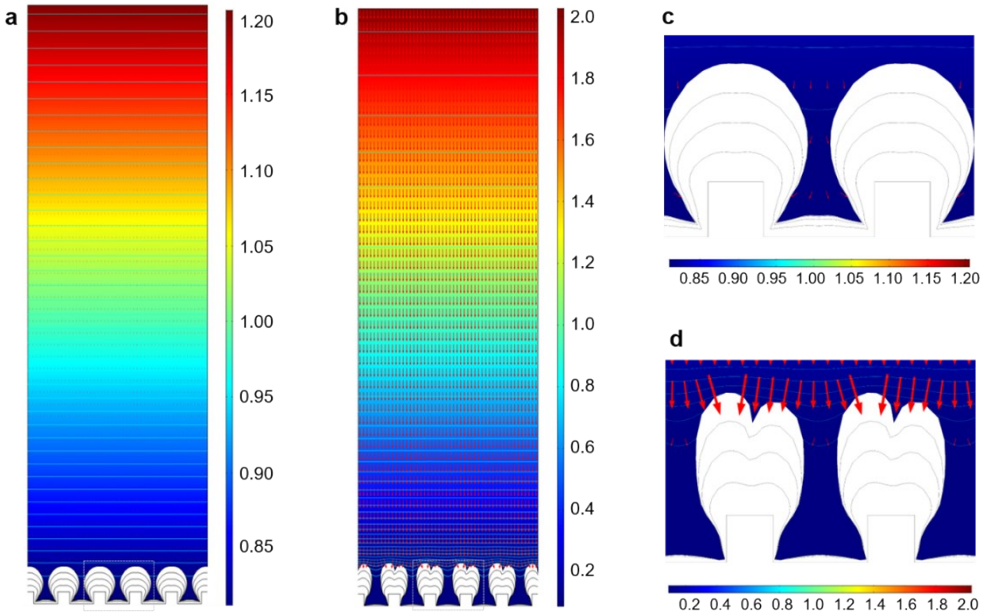

Figure S11. SEI effect on the normalized concentration distribution (color scale bar) inside domain and deposition geometries (bottom) after deposition at current densities of (a) (c) 0.2 mA/cm^2 and (b) (d) 1.0 mA/cm^2 for total capacities of 0.5 mAh/cm^2, 1.0 mAh/cm^2, 1.5 mAh/cm^2 and 2.0 mAh/cm^2, respectively. Figure (c) and (d) are the local deposition geometries from Figure (a) and (b).

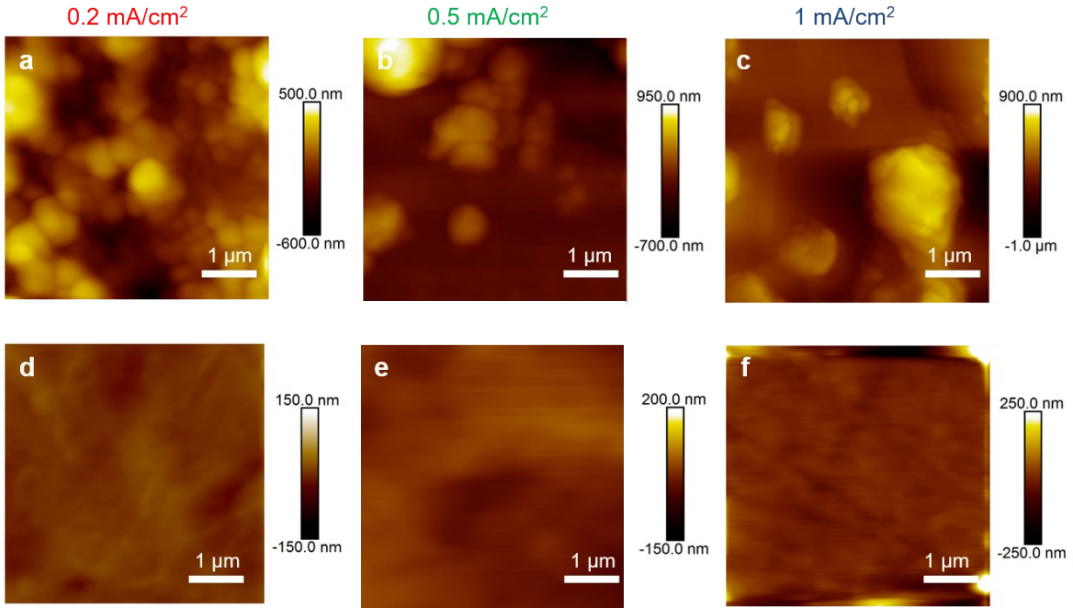

Figure S12. (a) (b) (c) The topological images corresponding to Figure 4 a-c. (d) (e) (f) The topological images corresponding to Figure 4 d-f.

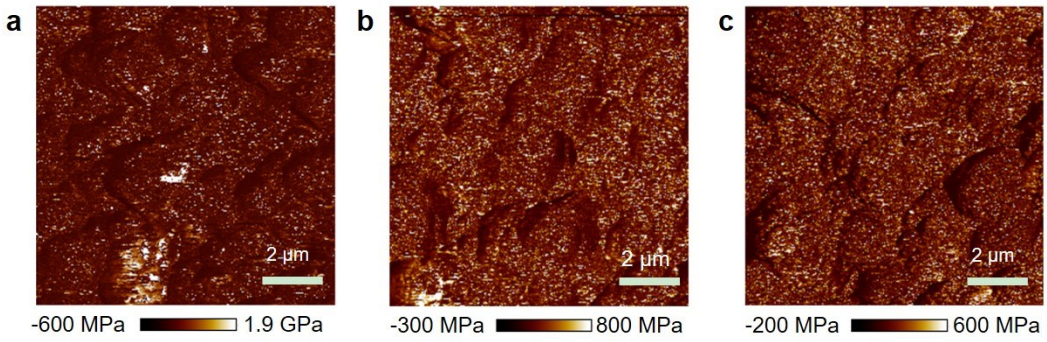

Figure S13. The modulus distribution maps of the as formed SEI after 1.0 mAh/cm^2 deposition at current densities of (a) 0.2 mA/cm^2, (b) 0.5 mA/cm^2 and (c) 1.0 mA/cm^2.

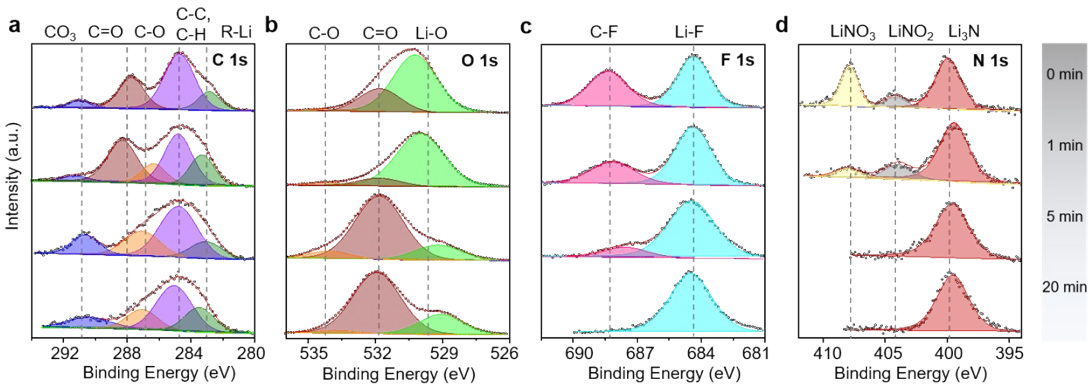

Figure S14. The composition of the SEI layer after deposition capacity of 1.0 mAh/cm^2 at 0.2 mA/cm^2. (a) C 1s, (b) O 1s, (c) F 1s and (d) N 1s.

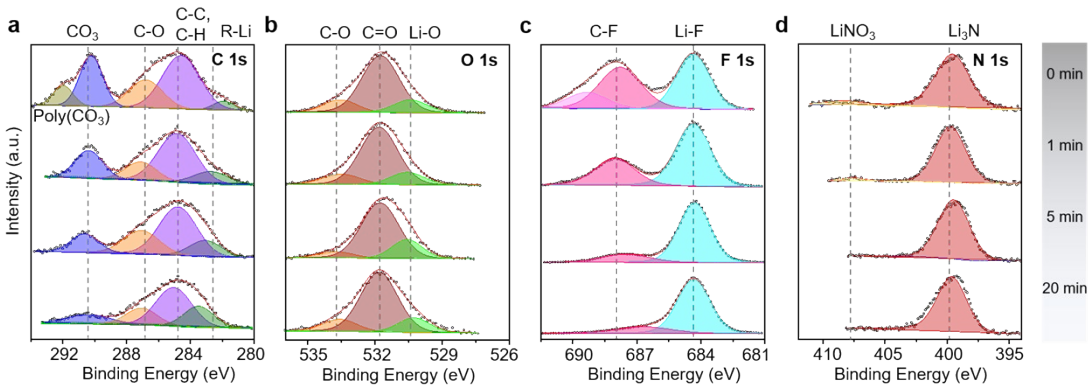

Figure S15. The composition of the SEI layer after deposition capacity of 1.0 mAh/cm^2 at 0.5 mA/cm^2. (a) C 1s, (b) O 1s, (c) F 1s and (d) N 1s.

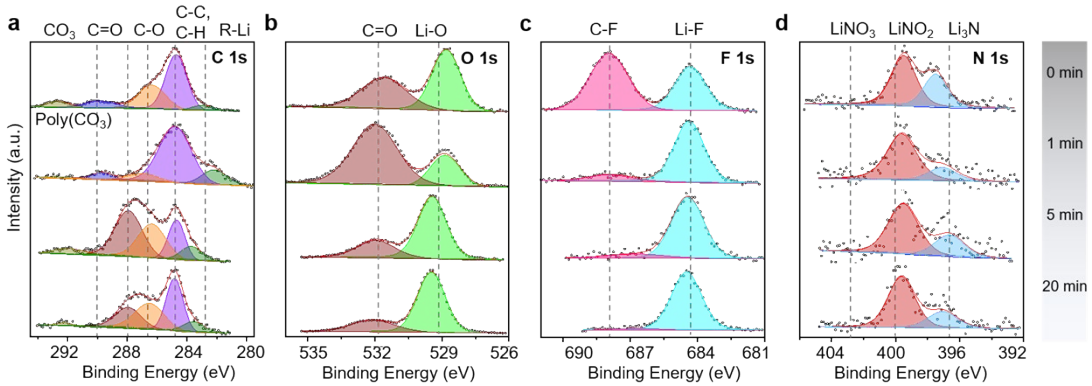

Figure S16. The composition of the SEI layer after deposition capacity of 1.0 mAh/cm^2 at 1.0 mA/cm^2. (a) C 1s, (b) O 1s, (c) F 1s and (d) N 1s.